THE JOURNAL OF BIOLOGICAL CHEMISTRY VOL. 287, NO. 52, pp. 43620–43629, December 21, 2012

Rho-associated Coiled-coil Kinase (ROCK) Protein Controls Microtubule Dynamics in a Novel Signaling Pathway That Regulates Cell Migration*[S]

Received for publication, June 24, 2012, and in revised form, October 22, 2012 Published, JBC Papers in Press, October 23, 2012, DOI 10.1074/jbc.M112.394965

Alice V. Schofield[‡¶], **Rohan Steel**[§], **and Ora Bernard**[‡¶1]

From the [‡]*St. Vincent's Institute of Medical Research Cytoskeleton and Cancer Unit and* [§]*Protein Chemistry and Metabolism Unit and from the* [¶]*Department of Medicine St. Vincent's Hospital, University of Melbourne, 3065 Victoria, Australia*

Background: ROCK regulates microtubule acetylation.
Results: ROCK phosphorylation of TPPP1/p25 inhibits the interaction between TPPP1 and HDAC6, resulting in increased HDAC6 deacetylation of microtubules, leading to increased cell motility.
Conclusion: ROCK phosphorylation of TPPP1 is a novel signaling pathway that regulates cell migration via increased HDAC6 activity and reduced MT acetylation.
Significance: This newly discovered ROCK/TPPP/HDAC6/MT signaling pathway might have important implications for cell motility and invasion.

The two members of the Rho-associated coiled-coil kinase (ROCK1 and 2) family are established regulators of actin dynamics that are involved in the regulation of the cell cycle as well as cell motility and invasion. Here, we discovered a novel signaling pathway whereby ROCK regulates microtubule (MT) acetylation via phosphorylation of the tubulin polymerization promoting protein 1 (TPPP1/p25). We show that ROCK phosphorylation of TPPP1 inhibits the interaction between TPPP1 and histone deacetylase 6 (HDAC6), which in turn results in increased HDAC6 activity followed by a decrease in MT acetylation. As a consequence, we show that TPPP1 phosphorylation by ROCK increases cell migration and invasion via modulation of cellular acetyl MT levels. We establish here that the ROCK-TPPP1-HDAC6 signaling pathway is important for the regulation of cell migration and invasion.

Rho-GTPase signaling is an important modulator of cytoskeletal dynamics via activation of its downstream effector kinases Rho-associated coiled-coil kinase (ROCK)[2] 1 and 2. ROCK phosphorylates a variety of substrates, most notably the actin regulatory proteins myosin light chain (MLC) (1), the LIM kinases (LIMK) (2–5) and myosin binding subunit of the MLC phosphatase (6) as well as the intermediate filament proteins desmin (7) and vimentin (8). Currently, very few microtubule (MT) regulatory ROCK substrates have been identified.

The dynamic reorganization of the MT network during cell division and migration relies on a precise balance between MT growth, stabilization, and depolymerization. Several known mechanisms modulate these events, including MT-associated proteins that promote MT polymerization and depolymerization, as well as MT posttranslational modifications, including phosphorylation, acetylation, polyglutamation, and detyrosination, that regulate MT stability. Importantly, acetylation of MTs correlates with polymer stabilization (9, 10). MT-bound α-tubulin subunits are reversibly acetylated on lysine 40 (Lys-40) by αTAT1 (11), MEC-17 (12), and the Elongator complex (13) acetyl transferases, whereas its deacetylation is regulated by histone deacetylase 6 (HDAC6) (14) and Sirtuin 2 (SIRT2) (15, 16).

It was suggested that tubulin acetylation is regulated by Rho-GTPase signaling. Treatment of cells with the Rho inhibitor C3 exoenzyme (17) or the ROCK inhibitor Y-27632 increases acetyl-MT levels (18–21), whereas overexpression of the constitutively active Rho mutant, Rho-V14, decreases its levels (17). Although it has been described that Rho regulates HDAC6 activity in osteoclasts via Rho-mediated inhibition of the HDAC6/mDia2 interaction that reduces its deacetylase activity (17), the role of ROCK signaling in the regulation of MT acetylation is yet to be elucidated.

TPPP1/p25 is a ubiquitously expressed 25-kDa protein belonging to the tubulin polymerization promoting protein (TPPP) family that includes TPPP2 (p20) and TPPP3 (p18) (22, 23). Overexpression of TPPP1 in cells promotes MT polymerization and an increase in MT acetylation, whereas introduction of TPPP1 RNAi reduces MT acetylation (24). TPPP1 regulates MT acetylation via binding to HDAC6 and inhibiting its activity (25). Recent reports suggest that *in vitro* TPPP1 activity is regulated by the ROCK substrates LIM kinase 1 and 2 (LIMK1 and 2) (24, 26).

We report here that ROCK-mediated phosphorylation of TPPP1 inhibits the TPPP1/HDAC6 interaction to drive a decrease in acetylated MT levels in cells, therefore resulting in increased cell migration and invasion.

* This research was supported by grants from the National Health and Medical Research Council (NHMRC), the Australian Research Council (ARC), the Cancer Council of Victoria, and in part by the Victorian Government Operational Infrastructure Support Program. This work was also supported by a fellowship from the NHMRC (to O. B.) and by an Australian Postgraduate Award and St. Vincent's Institute Foundation Top-up Scholarship (to A. V. S.).
[S] This article contains supplemental Fig 1.
[1] To whom correspondence should be addressed: St. Vincent's Institute of Medical Research, 9 Princes Street, Fitzroy, Victoria 3065, Australia. Tel.: 61-3-9288-2480; Fax: 61-3-9416-2676; E-mail: obernard@svi.edu.au.
[2] The abbreviations used are: ROCK, Rho-associated coiled-coil kinase; MLC, myosin light chain; MT, microtubule; Abs, antibodies; pMLC, phospho-myosin light chain; LIM, Lin-11, Isl-1, Mec-3.

EXPERIMENTAL PROCEDURES

Plasmid Constructs—pBABE-FLAG-TPPP1, pGEX4T1-GST-TPPP1, pEBG-GST-TPPP1 (24), pEBG-GST-LIMK1, and pEF-BOS-FLAG-LIMK1 (27) were described previously. Constitutively active pcDNA3-FLAG-ROCK1Δ4 (amino acids 1–477) and pcDNA-FLAG-ROCK1Δ4-K_D (amino acids 1–477, K105G) were a generous gift from Dr. S. Narumiya (Kyoto University, Japan). The TPPP1 alanine substitution mutations were introduced by whole plasmid PCR using PrimeSTAR HS DNA polymerase (Takara Bioscience) and the following primers: S32, 5′-AAGAGGCTGGCGCTGGAATCG-3′; S107, 5′-AAAGGGAAGGCTTGCCGGACC-3′; S159, 5′-AAAGCCATCGCGTCGCCCACA-3′; and antisense TPPP1, 5′-TGGCAGCTTTGGCAGGCTTG-3′ according to the manufacturer recommendations. The PCR products were digested with Dpn1. The constructs bearing the TPPP1 glutamic acid mutants were synthesized by Geneart (Invitrogen) and cloned into the BamH1 and Sal1 sites of the pBABE-FLAG-puro plasmid. LIMK2 was cloned into the BamH1 and Xho1 sites of the pEF-BOS-FLAG vector, and FLAG-ROCK1Δ4 was cloned into the baculovirus pFast-Bac-dual vector.

Cell Culture and Treatments—HEK293T and U2OS cells were maintained in DMEM supplemented with 10% (v/v) FBS at 37 °C in a humidified 5% CO_2 atmosphere. Sf-9 insect cells were maintained at 27 °C in SF900 II SFM (Invitrogen). The U2OS cell lines stably expressing TPPP1, TPPP1^{3Ala}, TPPP1^{3Glu} and vector were generated by infection with amphotropic retrovirus produced by cotransfection of pBABE-puro vector and an amphotropic helper plasmid. Viral supernatants supplemented with 8 μg/ml Polybrene were used to infect target cells. Transduced cells were selected with 2 μg/ml puromycin for 7 days.

Cells were treated with 10 μM of Y-27632 (Calbiochem) or DMSO vehicle for 16 h. When cells were stimulated with FBS, they were serum-starved for 24 h prior to the addition of 10% FBS for 30 min. Transfections were performed using the FuGENE 6 reagent (Roche) according to the protocol of the manufacturer. RNAi experiments were performed with ON-TARGETplus SMARTpool hTPPP1 or hLIMK2 siRNA or with the hLIMK1 siRNA 5′-TGGCAAGCGTGGACTTTCA-3′ (Dharmacon) using Lipofectamine 2000 (Invitrogen).

Metabolic Labeling of Cells with ^{32}P-orthophosphate—HEK293T or U2OS cells were transfected with FLAG-TPPP1 or GST-TPPP1 DNA constructs 24 h prior to incubation with RPMI 1640 without phosphate and L-glutamine (MP Biomedicals) for 16 h. 10 μM Y-27632 or vehicle was added 1 h prior to the addition of 0.1 mCi/ml ^{32}P-orthophosphate (MP Biomedicals) for 6 h. Immunoprecipitated or pulled-down phosphorylated TPPP1 and total cell extracts were analyzed by immunoblotting and autoradiography.

Protein Purification—The FLAG-ROCK1Δ4 protein was expressed and purified from Sf-9 insect cells. Briefly, bacmid FLAG-ROCK1Δ4 was generated by transformation of DH10Bac (Invitrogen) cells with pFast-FLAG-ROCK1Δ4 DNA according to the protocol of the manufacturer. The baculoviruses used to infect insect cells and express FLAG-ROCK1Δ4 were generated by transfection (Cellfectin® II, Invitrogen) of log-phase Sf-9 insect cells with recombinant bacmids. Constitutively active FLAG-ROCK1Δ4 was purified from Sf-9 cell pellets by resuspension in buffer (50 mM Tris-HCl (pH 7.5), 150 mM NaCl, and 0.1% Triton-X-100) and lysis in a French press at 10,000 p.s.i followed by centrifugation at 20,000 × *g* for 30 min. FLAG-ROCK1Δ4 was purified by incubation with anti-FLAG M2-agarose (Sigma) for 2 h at 4 °C, followed by 10 washes with resuspension buffer and elution with 1 μg/ml FLAG peptide (Sigma) for 30 min at room temperature. GST-TPPP1 and GST-cofilin proteins were expressed and purified from bacteria by incubation with glutathione-Sepharose 4B (GE Life Sciences). GST-LIMK1 was purified from HEK293T cells as described above. All proteins were dialyzed in TBS.

Immunoprecipitation—U2OS cell extracts were precleared with ~2 μg of isotype control and 30 μl of protein A- or G-Sepharose (Amersham Biosciences) for 1 h at 4 °C. Cleared lysates were incubated with ~2 μg of rat IgG2a, rat anti-TPPP1 mAb (24), mouse IgG or mouse anti-HDAC6 mAb, and 50 μl of protein A/G-Sepharose and incubated at 4 °C overnight. FLAG immunoprecipitation was performed as described above.

Immunoblotting—Membranes were probed overnight in 5% BSA with the following antibodies: anti-α-tubulin (1:5000), anti-acetyl-α-tubulin (1:5000), anti-pMLC Thr-18/Ser-19 (1:1000) (Cell Signaling Technology), anti-FLAG 9H1 mAb clone (28) (1:1000), anti-GST (1:3000) (Millipore), and anti-TPPP1 mAb or polyclonal antibodies (24).

In vitro Kinase Assays—*In vitro* kinase assays were performed at a molar ratio of 1:40 kinase:substrate. Proteins were incubated with 5 μCi [γ-^{32}P]ATP and 30 μM ATP in buffer containing 20 mM Hepes (pH 7.4), 10 mM $MgCl_2$, 10 mM NaF, 1 mM Na_3VO_4, and complete protease inhibitor tablet (Roche) at 37 °C for 10 min. Reactions in the presence of 5 μM Y-27632 or 100 nM 22j were preincubated for 10 min prior to the addition of ATP. Assays were analyzed by SDS-PAGE and followed by autoradiography.

Scratch-induced Migration and Invasion Assays—Wound closure assays were performed by scratching confluent cell monolayers preincubated with 10 μg/ml mitomycin C (Sigma) for 2 h with a pipette tip coated in 100% FBS. At 0 time and 18 h post-scratch, phase-contrast images were acquired. Matrigel invasion assays were performed with cells treated with mitomycin C as described above using growth factor-reduced BD Matrigel™ Basement Membrane Matrix (BD Biosciences) according to the recommendations of the manufacturer.

In vitro Tubulin Polymerization Assays—*In vitro* tubulin polymerization assays were performed using the tubulin polymerization assay kit (catalog no. BK006P, Cytoskeleton). Briefly, 2 μM of GST or GST-p25 was phosphorylated *in vitro* with purified FLAG-ROCK1Δ4 and 30 μM ATP. Reactions were mixed with general tubulin buffer (80 mM PIPES (pH 6.9), 2 mM $MgCl_2$, 0.5 mM EGTA), tubulin glycerol buffer (1 mM GTP with the addition of 5% glycerol), and 300 μg of purified tubulin. Tubulin turbidity was measured at 37 °C using a PolarSTAR optima plate reader configured to measure absorbance at $A_{340\ nm}$ every minute for 40 min with the plate shaking every 10 s.

Immunofluorescence Microscopy—Cells fixed in 100% methanol were blocked in 10% FBS prior to incubation with mouse anti-acetyl-α-tubulin (1:1000) and FITC-conjugated anti-α-tu-

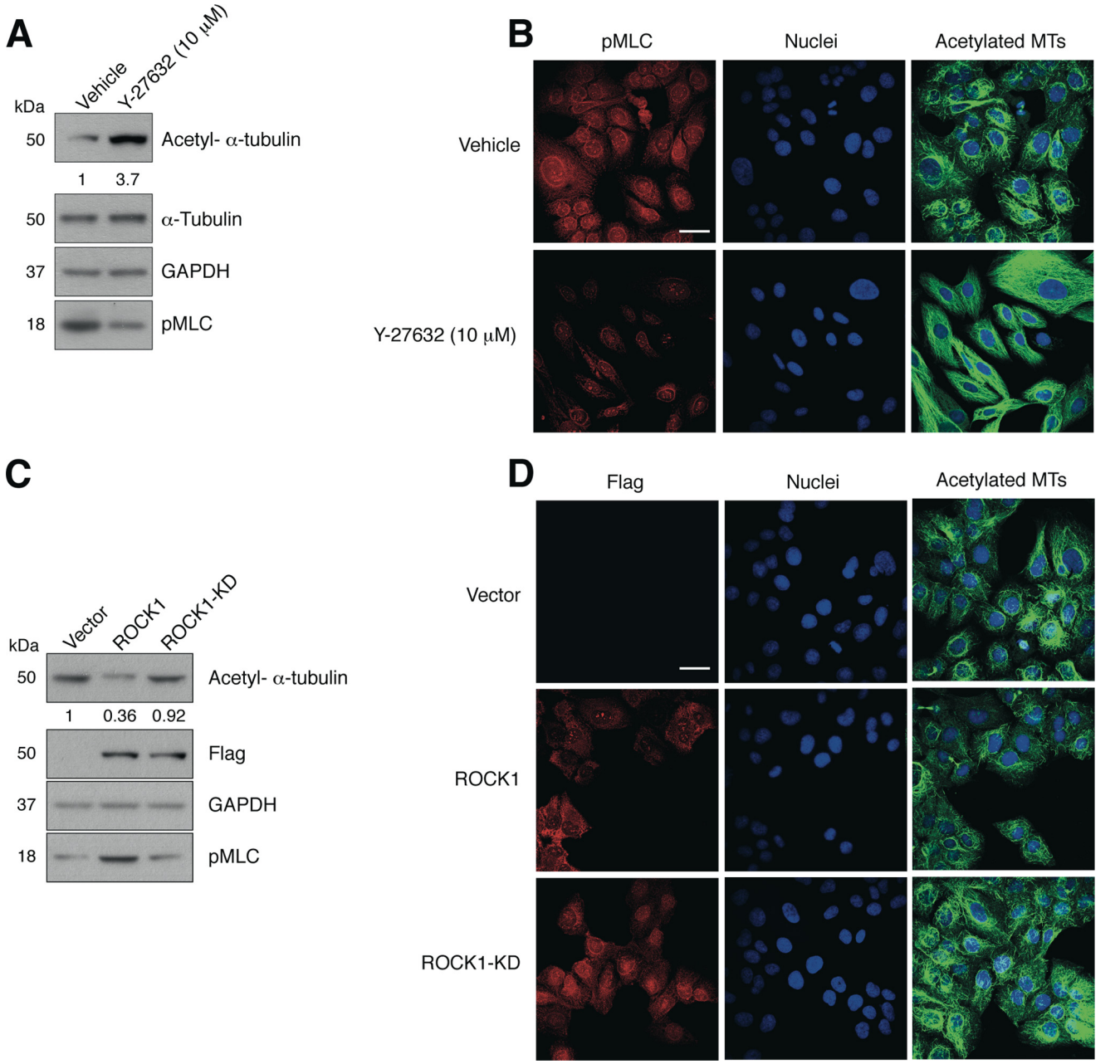

FIGURE 1. **ROCK regulates MT acetylation in U2OS cells.** U2SO cells treated with 10 μM Y-27632 or vehicle were lysed, and the levels of acetyl tubulin, α-tubulin, *p*MLC, and GAPDH were determined by immunoblotting (*A*) or by immunofluorescence microscopy after staining for *p*MLC (*red*), nuclei (*blue*), and acetylated MTs (*green*) (*B*). Immunoblots of lysates from U2OS cells transiently expressing constitutively active F-ROCK1 (50 kDa), F-ROCK1-K_D, or FLAG vector probed with anti-acetyl-tubulin, GAPDH (loading control), *p*MLC, and anti-FLAG Abs (*C*) and immunofluorescence microscopy (*D*). *Red*, FLAG; *blue*, nuclei; *green*, acetylated MTs. *Scale bar* = 50 μm.

bulin (1:200) (Sigma) antibodies. Cells were then incubated with Hoechst (1:10,000) and secondary Abs (anti-mouse Alexa Fluor 488 and anti-rat Alexa Fluor 594 (1:400)) (Invitrogen). Images were captured on a Nikon C1 confocal microscope.

Tandem MS/MS—GST-TPPP1 was digested from SDS-PAGE gel slices as described (29). Mass spectrometry was performed with an ABSciex tripleTOF equipped with a nano III source, running an information-dependent data acquisition program to fragment peptides, and the data were analyzed with Proteinpilot 4 software.

Data Analysis—Statistical analysis was performed with using two-tailed unpaired Student's *t*-tests.

RESULTS

ROCK Signaling Modulates Tubulin Acetylation—Inhibition of ROCK activity results in increased MT acetylation in cells (18–21). We therefore endeavored to identify the mechanism by which ROCK controls acetyl tubulin levels. First, we treated the U2OS osteosarcoma cell line with the ROCK inhibitor Y-27632 (10 μM) or vehicle and analyzed acetyl-α-tubulin levels by immunoblotting (Fig. 1*A*) and immunofluorescence microscopy (*B*). In accordance with data published previously, inhibition of ROCK activity, as confirmed by decreased phospho-MLC (*p*MLC) levels, resulted in increased cellular MT

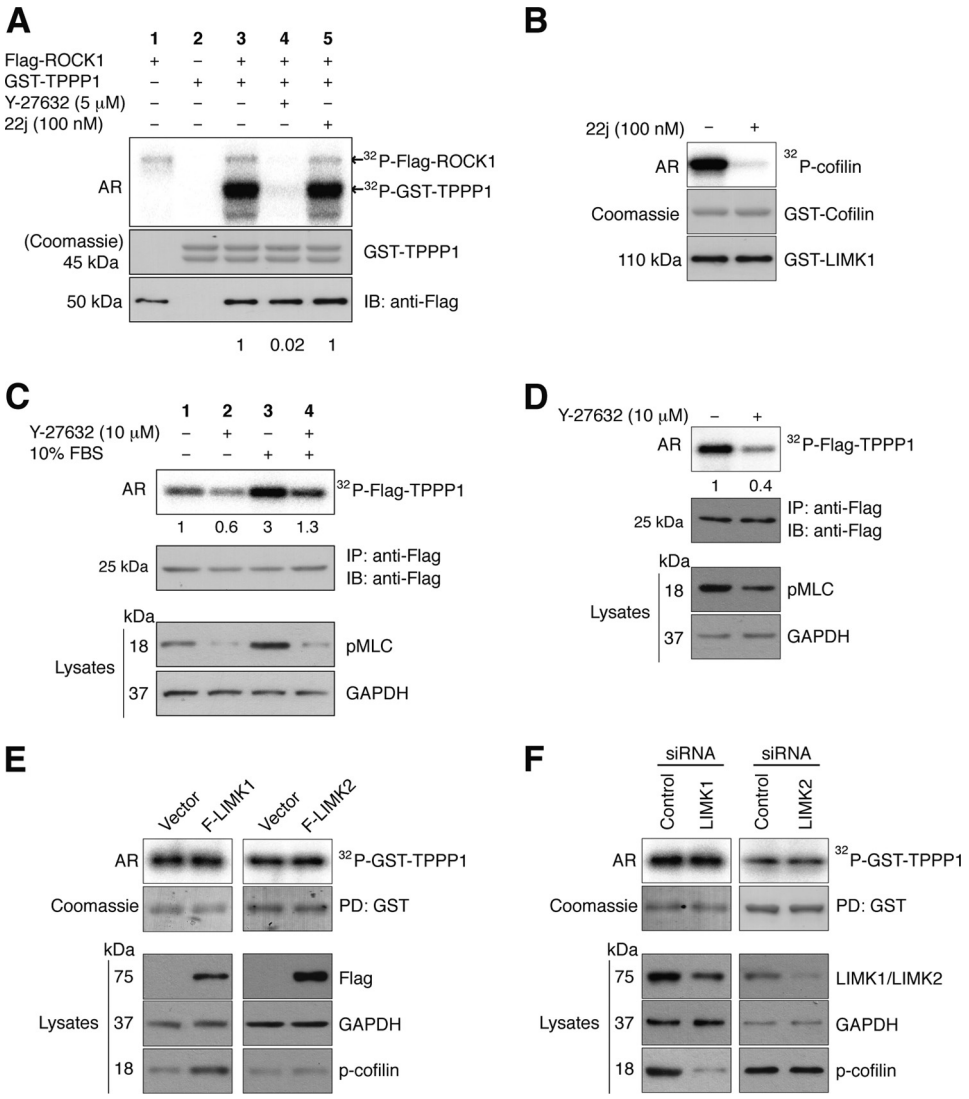

FIGURE 2. **ROCK phosphorylates TPPP1 *in vitro* and in cells.** *A*, TPPP1 is an *in vitro* ROCK1 substrate. ROCK1 (1 nM) and GST-TPPP1 (40 nM) were incubated in the presence of [^{32}P]γ-ATP (*lane 3*). Reactions were preincubated with the ROCK inhibitor Y-27632 (5 μM) (*lane 4*) or with the LIMK inhibitor 22j (100 nM) (*lane 5*). TPPP1 phosphorylation was analyzed by autoradiography (*AR*) (*top panel*). *IB*, immunoblot. *B,* 22j inhibits LIMK1-mediated cofilin phosphorylation. *In vitro* kinase assays were performed with GST-LIMK1 (1 nM) and GST-cofilin (40 nM) in the presence of 100 nM of 22j or vehicle (dimethyl sulfoxide) and analyzed as described. TPPP1 is phosphorylated by ROCK in cells. *C,* HEK293T cells transfected with F-TPPP1 were serum-starved (*lane 1*) in the presence of Y-27632 (10 μM) (*lane 2*) or stimulated with 10% FBS (*lane 3*) in the presence of Y-27632 (*lane 4*) and incubated with 0.1 mCi/ml ^{32}P-orthophosphate. Immunoprecipitated (*IP*) F-TPPP1 was analyzed by autoradiography (*top panel*) and immunoblotting (*bottom panels*). Lysates were blotted for *p*MLC as a control for ROCK activity. The numbers below the *top panel* represent the ratio between the values of *lanes 1* and *2* (0.6), *lanes 1* and *3* (3), and *lanes 1* and *4* (1.3). *D*, U2OS cells expressing F-TPPP1 were treated with Y-27632 (10 μM) or vehicle and analyzed as described in *C. D,* LIMK1 or LIMK2 do not phosphorylate TPPP1 in cells. HEK293T cells were transfected with GST-TPPP1 alone or together with F-LIMK1 (*left panels*) or F-LIMK2 (*right panels*) or (*E*) with LIMK1 or LIMK2 siRNA and metabolically labeled with ^{32}P-orthophosphate. GST-TPPP1 was pulled-down (*PD*) and analyzed by autoradiography and immunoblotting. Lysates were analyzed for LIMK1, LIMK2, GAPDH (loading control), and p-cofilin as a measure of LIMK activity.

acetylation. To further investigate the role of ROCK signaling in the regulation of MT acetylation, we transiently overexpressed the constitutively active FLAG-ROCK1Δ4 (ROCK1) or kinase dead ROCK1Δ4 (ROCK1-K_D) truncated proteins in U2OS cells. Overexpression of ROCK1 but not of ROCK1-K_D decreased acetyl-α-tubulin levels compared with the vector expressing cells, as shown by immunoblotting (Fig. 1*C*) and immunofluorescence microscopy (*D*). These results indicate that ROCK1 and/or its downstream effectors regulate MT acetylation in cells.

ROCK Phosphorylates TPPP1 in Vitro and in Cells—MT acetylation is regulated by two deacetylases, HDAC6 and SIRT2. HDAC6 activity is inhibited through its interaction with TPPP1, resulting in increased MT acetylation (25). We therefore hypothesized that ROCK phosphorylation of TPPP1 affects its interaction with HDAC6. To test this hypothesis, we first examined whether TPPP1 is a ROCK substrate. *In vitro* kinase assays with GST-TPPP1 and FLAG-ROCK1 (F-ROCK1) showed that TPPP1 was efficiently phosphorylated by ROCK1 (Fig. 2*A*, *lane 3*). To confirm that TPPP1 was specifically phosphorylated by ROCK1 and not by contaminating kinases, the kinase reactions were preincubated with the ROCK inhibitor Y-27632 (5 μM) or vehicle. Inhibition of ROCK activity abolished TPPP1 phosphorylation (Fig. 2*A*, *lane 4*), suggesting that TPPP1 is a direct substrate of ROCK1 *in vitro*. Moreover, we performed the reaction in the presence of the LIMK inhibitor

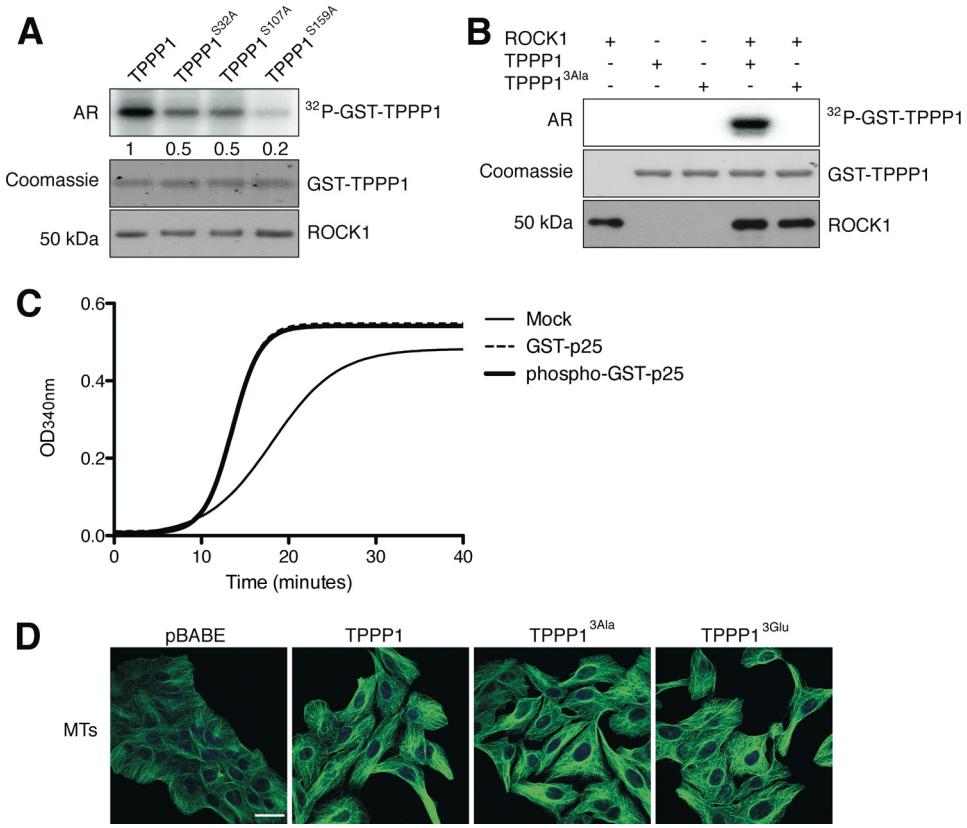

FIGURE 3. **TPPP1 phosphorylation on Ser-32, Ser-159, and Ser-107 *in vivo* and *in vitro* by ROCK does not alter its MT polymerizing activity.** *A*, *in vitro* kinase assay showing that the phosphorylation of the TPPP1^{S32A}, TPPP1^{S107A}, and TPPP1^{S159A} proteins by ROCK1Δ4 (ROCK1) is reduced in comparison with that of TPPP1 (*top panel*). The numbers below the *top panel* represent the ratio between the phosphorylation level of wild-type TPPP1 and that of the single TPPP1 mutants. *AR*, autoradiography. *B*, the triple S32A/S107A/S159A mutations abolished TPPP1 phosphorylation by ROCK1. *C*, *in vitro* tubulin polymerization assay in the presence of bacterially purified GST-TPPP1 and *in vitro* ROCK1 phosphorylated GST-TPPP1. *D*, overexpression of TPPP1, TPPP1^{3Ala}, or TPPP1^{3Glu} in U2OS cells increased MT levels (*green*) as shown by immunofluorescence microscopy (nuclei, *blue*). *Scale bar* = 50 μm.

22j (30), as it was suggested that the LIMKs phosphorylate TPPP1 (24, 26)). We showed that although inhibition of LIMK activity decreased the phosphorylation of its substrate cofilin (Fig. 2*B*), the level of TPPP1 phosphorylation by ROCK was unchanged (*A*, *lane 5*), therefore confirming that TPPP1 is phosphorylated by ROCK *in vitro*.

To confirm that TPPP1 is also an *in vivo* ROCK substrate, we analyzed the effect of ROCK inhibition on TPPP1 phosphorylation in cells. We metabolically labeled HEK293T or U2OS cells overexpressing FLAG-TPPP1 (F-TPPP1) with ^{32}P-orthophosphate in the presence or absence of 10 μM Y-27632. We demonstrated that inhibition of ROCK activity, demonstrated by decreased pMLC levels in cell lysates, significantly decreased TPPP1 phosphorylation compared with the controls in HEK293T (Fig. 2*C Lanes 1* and 2) as well as in U2OS cells (Fig. 2*D*). Furthermore, although TPPP1 phosphorylation was greatly increased in cells stimulated with 10% FBS (3-fold) (Fig. *2C*, *lanes 1* and *3*), inhibition of ROCK activity in FBS-stimulated cells reduced TPPP1 phosphorylation 2-fold in comparison to FBS only-treated cells (*C*, *lanes 3* and *4*). These results strongly suggest that TPPP1 is phosphorylated by ROCK, not only *in vitro* but also in cells.

To rule out the possibility that the ROCK-activated kinases LIMK1 and 2 are responsible for the phosphorylation of TPPP1 *in vivo*, which has been suggested previously (24, 26), we labeled HEK293T cells overexpressing FLAG-LIMK1 (F-LIMK1), FLAG-LIMK2 (F-LIMK2), or vector control with ^{32}P-orthophosphate and analyzed the level of TPPP1 phosphorylation. Overexpression of LIMK1 or 2 did not alter the level of TPPP1 phosphorylation, despite increased phosphorylation of their established substrate cofilin (Fig. 2*E*). Furthermore, RNAi-mediated down-regulation of LIMK1 or LIMK2 levels had no effect on TPPP1 phosphorylation (Fig. 2*F*). Overall, these results indicate that ROCK phosphorylates TPPP1 directly *in vitro* and in cells.

ROCK Phosphorylates TPPP1 on Ser-32, Ser-107, and Ser-159—We next identified the TPPP1 phosphorylation sites. Initially, we characterized TPPP1 phosphorylation stoichiometry, which revealed that it was phosphorylated on three serine residues by ROCK (data not shown). Subsequently, we analyzed the *in vivo* TPPP1 phosphorylation sites by MS/MS and identified that TPPP1 is phosphorylated on three potential ROCK phosphorylation motifs (R/K*XX*S/T or R/K*X*S/T) (31, 32) in cells: Ser-32, Ser-107, and Ser-159 (data not shown).

To confirm that these TPPP1 sites are phosphorylated by ROCK, we generated mutants bearing single alanine substitutions and performed *in vitro* kinase assays with F-ROCK1. Fig. 3*A* demonstrates that a single mutation of Ser-32, Ser-107, or Ser-159 results in decreased TPPP1 phosphorylation as compared with their wild-type counterpart. We therefore generated a triple TPPP1 S32A/S107A/S159A mutant construct, designated here as TPPP1^{3Ala}. *In vitro* kinase assays with this tri-

alanine TPPP1 mutant completely abolished TPPP1 phosphorylation by ROCK1 (Fig. 3*B*, *top panel*), thereby confirming that ROCK1 phosphorylates TPPP1 on Ser-32, Ser-107, and Ser-159.

ROCK Phosphorylation of TPPP1 Does Not Alter Its MT Polymerizing Activity—TPPP1 has two established cellular functions. It promotes MT polymerization and regulates HDAC6 activity (25, 33). To evaluate the impact of TPPP1 phosphorylation by ROCK on its MT polymerization activity, we performed *in vitro* MT polymerization assays with bacterially purified GST-TPPP1 that was phosphorylated *in vitro* with F-ROCK1. Both the wild-type and the ROCK1 phosphorylated GST-TPPP1 increased the rate and level of MT polymerization compared with spontaneous MT polymerization (Fig. 3*C*), therefore suggesting that TPPP1 phosphorylation by ROCK does not alter its MT polymerizing activity.

To confirm this in cells, we established stable U2OS cell lines expressing F-TPPP1, F-TPPP1^{3Ala}, F-TPPP1^{3Glu} (phospho-mimetic mutant), or vector alone and analyzed their MT network by staining with anti-α-tubulin Abs, followed by immunofluorescence microscopy. Overexpression of all three TPPP1 proteins resulted in increased MT levels compared with the vector-expressing cells (Fig. 3*D*), confirming that TPPP1 phosphorylation by ROCK does not alter its MT polymerizing activity.

ROCK Phosphorylation of TPPP1 Inhibits its HDAC6 Regulatory Activity—We next evaluated the impact of TPPP1 phosphorylation by ROCK on its HDAC6 regulatory activity. TPPP1 modulates HDAC6 activity via an inhibitory binding mechanism (25). Therefore, we initially analyzed the impact of Y-27632 treatment of U2OS cells on the interaction between endogenous HDAC6 and TPPP1 proteins. We first immunoprecipitated TPPP1 from these lysates and analyzed its ability to coprecipitate HDAC6. Inhibition of ROCK activity increased the interaction between TPPP1 and HDAC6 compared with vehicle-treated cells (Fig. 4*A*). Similarly, immunoprecipitation of endogenous HDAC6 from these lysates demonstrated that inhibition of ROCK activity increased its ability to interact with TPPP1 (Fig. 4*B*).

ROCK Phosphorylation of TPPP1 Results in Increased MT Acetylation—We have demonstrated that ROCK-mediated phosphorylation of TPPP1 inhibits its HDAC6 binding resulting in increased HDAC6 activity. To confirm these results, we analyzed the interaction between endogenous HDAC6 and wild-type F-TPPP1, F-TPPP1^{3Ala}, or F-TPPP1^{3Glu} overexpressed in U2OS cells. F-TPPP1 immunoprecipitation demonstrated that TPPP1 and TPPP1^{3Ala} interacted with HDAC6, with TPPP1^{3Ala} exhibiting a higher binding affinity to HDAC6 (Fig. 4*C*). In contrast, F-TPPP1^{3Glu} did not interact with HDAC6. Similarly, immunoprecipitation of HDAC6 revealed that it interacts with F-TPPP1 and F-TPPP1^{3Ala} but not with F-TPPP1^{3Glu} (Fig. 4*D*). The interaction between HDAC6 and TPPP1 is less efficient than the interaction between HDAC6 and F-TPPP1^{3Ala}, suggesting that wild-type TPPP1 is partially phosphorylated in cells. These results indicate that phosphorylation of TPPP1 by ROCK inhibits its binding to HDAC6.

To show that increased HDAC6 activity leads to increased tubulin deacetylation in U2OS cells overexpressing the TPPP1 proteins described above, we performed a Western blot analysis for acetyl-α-tubulin. Expression of TPPP1 and TPPP1^{3Ala} increased acetyl-α-tubulin levels (Fig. 4*E*), whereas acetyl-α-tubulin levels in cells expressing TPPP1^{3Glu}, which mimics phospho-TPPP1, remained similar to that of vector-expressing cells. Immunofluorescence staining of acetylated MTs confirmed that both TPPP1 and TPPP1^{3Ala} expression increased acetylated MT levels compared with control cells, whereas expression of TPPP1^{3Glu} had no effect (Fig. 4*F*).

Taken together, these results clearly demonstrate that phosphorylation of TPPP1 by ROCK inhibits its interaction with HDAC6, thereby resulting in increased HDAC6 activity in cells, without altering TPPP1-mediated regulation of MT polymerization.

TPPP1 Regulates Cell Migration and Invasion—It is well established that MT acetylation is involved in the regulation of cell migration (34). Therefore, we next characterized the role of the ROCK-TPPP1-HDAC6 signaling pathway in cell migration and invasion. We first analyzed cell migration by performing scratch-induced wound healing migration assays. Overexpression of TPPP1 significantly reduced wound-closure 18 h post-wounding compared with the control cells (Fig. 5, *A* and *B*). Similarly, overexpression of TPPP1^{3Ala} significantly reduced cell migration compared with both control and wild-type TPPP1 expressing cells, which is likely due to partial wild-type TPPP1 phosphorylation. In contrast, expression of TPPP1^{3Glu} increased wound healing compared with control cells (Fig. 5, *A* and *B*), suggesting that TPPP1 MT polymerizing activity contributes to cell migration. Finally, we compared the migration of U2OS cells transfected with TPPP1 or control siRNAs. Knockdown of TPPP1 significantly increased wound closure compared with controls (Fig. 5, *C* and *D*). These results clearly suggest that TPPP1-mediated regulation of HDAC6 activity leads to the inhibition of cell migration. Further analysis of the role of ROCK signaling in U2OS cell migration revealed that overexpression of ROCK increased wound-closure, whereas inhibition of its activity reduced wound-closure rates (supplemental Fig. 1, *A–D*). Therefore, we confirm that ROCK-mediated modulation of the TPPP1/HDAC6 interaction is important for the regulation of cell migration.

To study the role of TPPP1 in cell invasion, we performed Matrigel invasion assays and analyzed the migration of stable U2OS cells through Basement Membrane. Overexpression of TPPP1 and TPPP1^{3Ala} significantly reduced the invasiveness of these cells compared with the control (Fig. 5*E*), whereas overexpression of TPPP1^{3Glu} significantly increased their invasiveness. Furthermore, knockdown of TPPP1 significantly increased the invasiveness of cells (Fig. 5*F*). Similarly, ROCK overexpression and inhibition increase and decrease cell invasion, respectively (supplemental Fig. 1, *E* and *F*). These results demonstrate that TPPP1, via ROCK phosphorylation, regulates cell migration and invasion through its dual regulation of MT polymerization and HDAC6 activity.

DISCUSSION

We describe here a novel signaling pathway initiated by ROCK phosphorylation of TPPP1. This pathway, which includes ROCK-TPPP1-HDAC6, leads to increased HDAC6

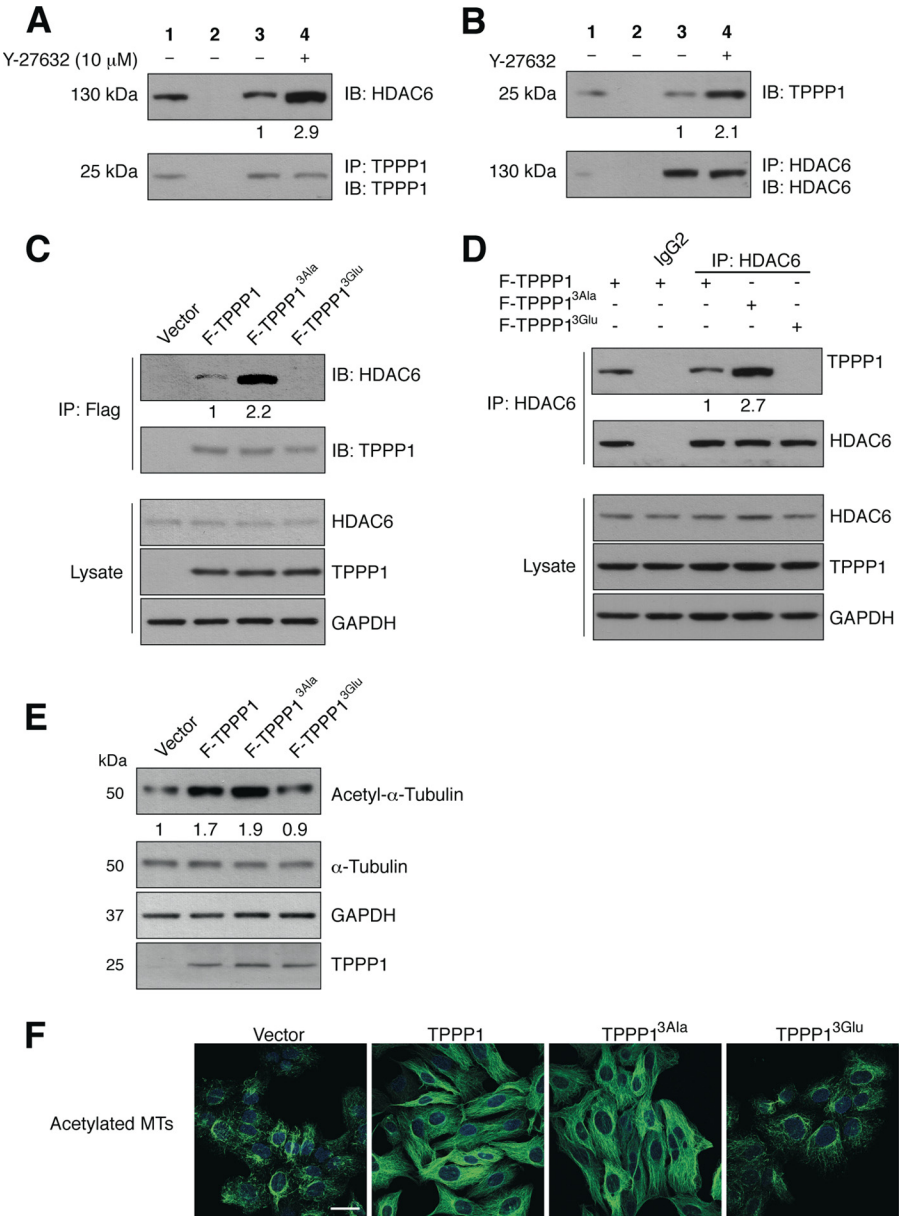

FIGURE 4. **ROCK phosphorylation of TPPP1 inhibits HDAC6 binding and tubulin acetylation.** *A*, inhibition of ROCK activity increases the interaction between TPPP1 and HDAC6. U2OS cell extracts treated with Y-27632 (*lane 4*) or vehicle (*lane 3*) were incubated with IgG (*lane 2*) or rabbit anti-TPPP1 polyclonal Abs (*lanes 3* and *4*). The immunoprecipitated proteins (*IP*) and total cell extracts were analyzed by immunoblotting (*IB*) for TPPP1 and HDAC6. *B*, immunoblots of extracts from *A* immunoprecipitated with mouse anti-HDAC6 mAb and probed as in *A*. *C*, ROCK phosphorylation of TPPP1 inhibits its binding to HDAC6. Extracts from U2OS cells expressing F-TPPP1 and its mutants were purified with anti-FLAG M2-agarose, and total lysates and IP were immunoblotted and probed with anti-HDAC6 and anti-FLAG mAbs. *D*, cell extracts from *C* were immunoprecipitated with anti-HDAC6 or IgG Abs. Total lysates and IPs were analyzed by immunoblotting as in *C*. *E*, immunoblot of lysates from U2OS cells stably expressing F-TPPP1 and its mutants were analyzed for acetyl tubulin, α-tubulin, GAPDH (loading control), and F-TPPP1. *F*, the U2OS cell lines described in *E* were stained for nuclei (*blue*) and acetylated MTs (*green*) and analyzed by immunofluorescence microscopy. *Scale bar* = 50 mm. The numbers below the *top panels in A*, *B*, *D*, and *E* represent the fold changes in the indicated protein levels.

activity, resulting in decreased MT acetylation. Overall, the activation of this novel pathway by ROCK results in enhanced cell motility and invasion via decreased tubulin acetylation (Fig. *6*).

ROCK1 and 2 have a large number of substrates and are important regulators of the actin cytoskeleton through phosphorylation of the LIMKs, MLC, and the myosin-binding subunit of the MLC phosphatase. Here we identified a novel MT regulatory ROCK substrate, TPPP1. TPPP1 is phosphorylated *in vitro* and in cells on multiple sites. These sites are phosphorylated *in vitro* by CDK5, ERK2, and protein kinase A, but only TPPP1 phosphorylation by ERK2 inhibited its tubulin polymerization activity (35). We show that TPPP1 phosphorylation by ROCK has no effect on its tubulin polymerizing activity, suggesting that the conformational changes induced by ROCK phosphorylation do not alter its interaction with MTs. We also clearly demonstrate that ROCK1, and not the LIMKs, is responsible for TPPP1 phosphorylation, as claimed previously (24, 26). As the ROCKs strongly interact and copurify with the LIMKs, the previously published findings are likely to reflect TPPP1 phosphorylation by ROCK but not by LIMKs, as demonstrated in this study.

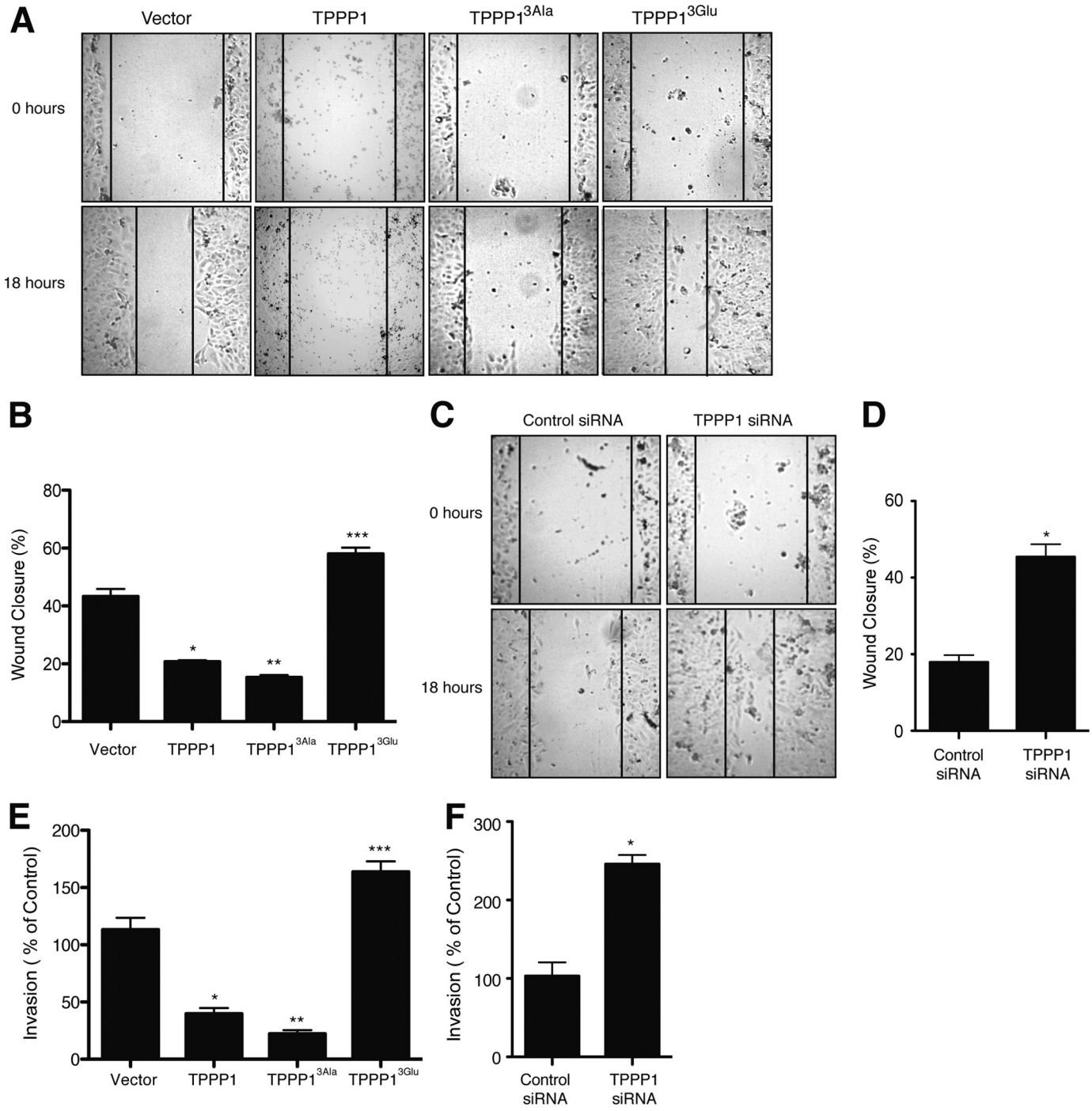

FIGURE 5. **TPPP1 inhibition of cell migration and invasion is relieved by its phosphorylation by ROCK.** *A*, scratch-induced migration assay. Confluent U2OS stable cell lines were scratched with pipette tips. Phase contrast microscope images were taken at 0 and 18 h post-wound induction. *B*, graphical representation of wound closure displayed in *A* ($n = 3$; *, $p = 0.001$; **, $p = 0.0005$; ***, $p = 0.0116$). *C*, scratch-induced migration assay of U2OS cells transiently transfected with TPPP1 or control siRNA. *D*, graphical representation of the wound closure rate of cells in *C* ($n = 3$; *, $p = 0.0019$). TPPP1 regulates cell invasion. *E*, Matrigel invasion assay with stable U2OS cells expressing TPPP1 proteins as indicated ($n = 3$; *, $p = 0.0031$; **, $p = 0.0011$; ***, $p = 0.022$). *F*, invasion assay performed with U2OS cells transiently transfected with TPPP1 or control siRNA ($n = 3$; *, $p = 0.0024$).

The interaction between TPPP1 and HDAC6 results in the inhibition of HDAC deacetylase activity and, therefore, increased MT acetylation. We show here that phosphorylation of TPPP1 by ROCK prevents its interaction with HDAC6, resulting in an increase in its deacetylase activity. Our findings establish, for the first time, that ROCK signaling regulates tubulin acetylation through its phosphorylation of TPPP1. These findings reveal a mechanism by which ROCK regulates MT acetylation and confirm previous studies demonstrating that Rho-ROCK inhibition increases acetyl-α-tubulin levels (18–21), whereas Rho activation decreases it (17).

Tubulin acetylation is very important for many cellular processes, including cell migration and invasion. Previous studies linked increased tubulin acetylation with reduced cell motility

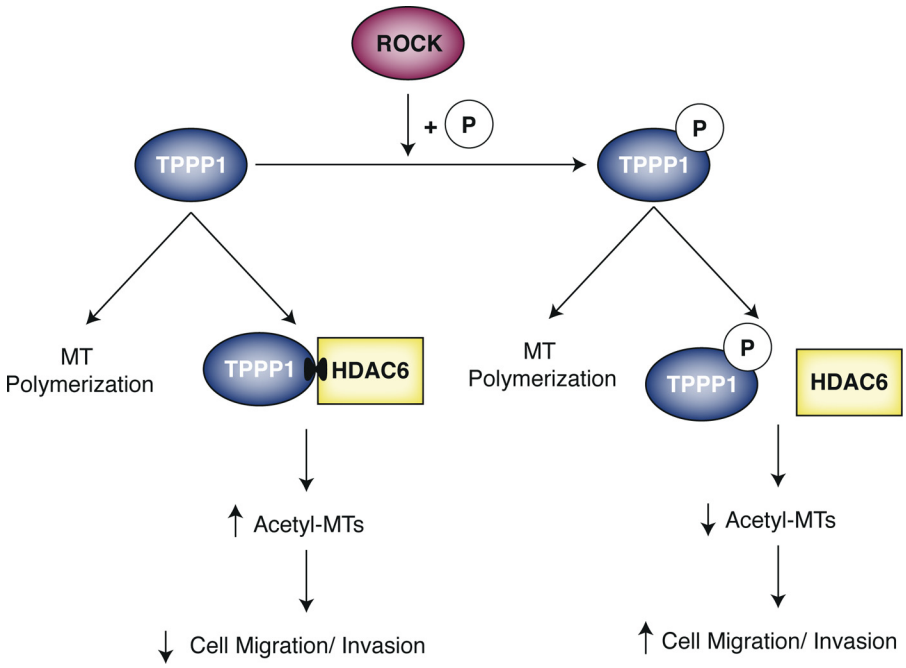

FIGURE 6. **TPPP1 regulates the microtubule network.** TPPP1 regulates the microtubule network by promoting tubulin polymerization and by binding to HDAC6 to inhibit its activity. This leads to increased acetylation of the HDAC6 substrates α-tubulin. Increased MT acetylation results in decreased cell migration and invasion. When TPPP1 is phosphorylated by ROCK, it is unable to bind to HDAC6, resulting in increased HDAC6 activity in the cell, which leads to decreased acetylated-tubulin levels and increased cell migration and invasion.

and invasion (36, 37), whereas overexpression of HDAC6, which reduced tubulin acetylation, increased their invasiveness (38), thereby suggesting that aberrant tubulin acetylation may contribute to malignancies. Our data establish that overexpression of TPPP1 reduces cell migration and invasion, whereas its down-regulation increases cell migration and invasion. Similarly, ROCK-mediated TPPP1 phosphorylation, which inhibits its interaction of HDAC6, thus resulting in reduced MT acetylation, increases cell migration and invasion. Although it is likely that TPPP1-mediated regulation of tubulin acetylation is primarily responsible for its regulation of cell migration, it cannot be ruled out that dual regulation of HDAC6 and tubulin polymerization by TPPP1 contribute to decreased cell migration. Our studies and those of others show that activation of ROCK contributes to increased cell migration and invasion (39) and that inhibition of ROCK signaling inhibits cell migration (40), therefore strengthening our observation that ROCK-TPPP1 signaling increases cell migration.

In conclusion, our work has identified TPPP1 as a novel ROCK substrate. When TPPP1 is phosphorylated by ROCK, it is unable to bind to HDAC6 and inhibit its activity, resulting in a decreased cellular level of acetylated tubulin and increased cell migration (Fig. 6).

Acknowledgments—We thank Dr. Rong Li and Dr. Guizhi Sun (Monash Immunology and Stem Cell Laboratories (MISCL), Monash University) for technical assistance or providing reagents, respectively, and Dr. Bryce Harrison (Lexicon) for the generous gift of 22j. We also thank Prof. Claude Bernard (MISCL, Monash University) and Drs. Boris Sarcevic and Jörg Heierhorst for providing reagents and critical reading of the manuscript.

REFERENCES

1. Amano, M., Ito, M., Kimura, K., Fukata, Y., Chihara, K., Nakano, T., Matsuura, Y., and Kaibuchi, K. (1996) Phosphorylation and activation of myosin by Rho-associated kinase (Rho-kinase). *J. Biol. Chem.* **271,** 20246–20249
2. Ohashi, K., Nagata, K., Maekawa, M., Ishizaki, T., Narumiya, S., and Mizuno, K. (2000) Rho-associated kinase ROCK activates LIM-kinase 1 by phosphorylation at threonine 508 within the activation loop. *J. Biol. Chem.* **275,** 3577–3582
3. Maekawa, M., Ishizaki, T., Boku, S., Watanabe, N., Fujita, A., Iwamatsu, A., Obinata, T., Ohashi, K., Mizuno, K., and Narumiya, S. (1999) Signaling from Rho to the actin cytoskeleton through protein kinases ROCK and LIM-kinase. *Science* **285,** 895–898
4. Katoh, K., Kano, Y., Amano, M., Kaibuchi, K., and Fujiwara, K. (2001) Stress fiber organization regulated by MLCK and Rho-kinase in cultured human fibroblasts. *Am. J. Physiol. Cell Physiol.* **280,** C1669–1679
5. Sumi, T., Matsumoto, K., and Nakamura, T. (2001) Specific activation of LIM kinase 2 via phosphorylation of threonine 505 by ROCK, a Rho-dependent protein kinase. *J. Biol. Chem.* **276,** 670–676
6. Kimura, K., Ito, M., Amano, M., Chihara, K., Fukata, Y., Nakafuku, M., Yamamori, B., Feng, J., Nakano, T., Okawa, K., Iwamatsu, A., and Kaibuchi, K. (1996) Regulation of myosin phosphatase by Rho and Rho-associated kinase (Rho-kinase) *Science* **273,** 245–248
7. Inada, H., Goto, H., Tanabe, K., Nishi, Y., Kaibuchi, K., and Inagaki, M. (1998) Rho-associated kinase phosphorylates desmin, the myogenic intermediate filament protein, at unique amino-terminal sites. *Biochem. Biophys. Res. Commun.* **253,** 21–25
8. Matsuzawa, K., Kosako, H., Inagaki, N., Shibata, H., Mukai, H., Ono, Y., Amano, M., Kaibuchi, K., Matsuura, Y., Azuma, I., and Inagaki, M. (1997) Domain-specific phosphorylation of vimentin and glial fibrillary acidic protein by PKN. *Biochem. Biophys. Res. Commun.* **234,** 621–625
9. Maruta, H., Greer, K., and Rosenbaum, J. L. (1986) The acetylation of α-tubulin and its relationship to the assembly and disassembly of microtubules. *J. Cell Biol.* **103,** 571–579
10. Piperno, G., LeDizet, M., and Chang, X. J. (1987) Microtubules containing acetylated α-tubulin in mammalian cells in culture. *J. Cell Biol.* **104,** 289–302

11. Shida, T., Cueva, J. G., Xu, Z., Goodman, M. B., and Nachury, M. V. (2010) The major α-tubulin K40 acetyltransferase αTAT1 promotes rapid ciliogenesis and efficient mechanosensation. *Proc. Natl. Acad. Sci. U.S.A.* **107,** 21517–21522
12. Akella, J. S., Wloga, D., Kim, J., Starostina, N. G., Lyons-Abbott, S., Morrissette, N. S., Dougan, S. T., Kipreos, E. T., and Gaertig, J. (2010) MEC-17 is an α-tubulin acetyltransferase. *Nature* **467,** 218–222
13. Creppe, C., Malinouskaya, L., Volvert, M. L., Gillard, M., Close, P., Malaise, O., Laguesse, S., Cornez, I., Rahmouni, S., Ormenese, S., Belachew, S., Malgrange, B., Chapelle, J. P., Siebenlist, U., Moonen, G., Chariot, A., and Nguyen, L. (2009) Elongator controls the migration and differentiation of cortical neurons through acetylation of α-tubulin. *Cell* **136,** 551–564
14. Hubbert, C., Guardiola, A., Shao, R., Kawaguchi, Y., Ito, A., Nixon, A., Yoshida, M., Wang, X. F., and Yao, T. P. (2002) HDAC6 is a microtubule-associated deacetylase. *Nature* **417,** 455–458
15. North, B. J., Marshall, B. L., Borra, M. T., Denu, J. M., and Verdin, E. (2003) The human Sir2 ortholog, SIRT2, is an NAD+-dependent tubulin deacetylase. *Mol. Cell* **11,** 437–444
16. Reed, N. A., Cai, D., Blasius, T. L., Jih, G. T., Meyhofer, E., Gaertig, J., and Verhey, K. J. (2006) Microtubule acetylation promotes kinesin-1 binding and transport. *Curr. Biol.* **16,** 2166–2172
17. Destaing, O., Saltel, F., Gilquin, B., Chabadel, A., Khochbin, S., Ory, S., and Jurdic, P. (2005) A novel Rho-mDia2-HDAC6 pathway controls podosome patterning through microtubule acetylation in osteoclasts. *J. Cell Sci.* **118,** 2901–2911
18. Kadir, S., Astin, J. W., Tahtamouni, L., Martin, P., and Nobes, C. D. (2011) Microtubule remodelling is required for the front-rear polarity switch during contact inhibition of locomotion. *J. Cell Sci.* **124,** 2642–2653
19. Takesono, A., Heasman, S. J., Wojciak-Stothard, B., Garg, R., and Ridley, A. J. (2010) Microtubules regulate migratory polarity through Rho/ROCK signaling in T cells. *PLoS ONE* **5,** e8774
20. Belletti, B., Pellizzari, I., Berton, S., Fabris, L., Wolf, K., Lovat, F., Schiappacassi, M., D'Andrea, S., Nicoloso, M. S., Lovisa, S., Sonego, M., Defilippi, P., Vecchione, A., Colombatti, A., Friedl, P., and Baldassarre, G. (2010) p27kip1 controls cell morphology and motility by regulating microtubule-dependent lipid raft recycling. *Mol. Cell Biol.* **30,** 2229–2240
21. Birukova, A. A., Birukov, K. G., Smurova, K., Adyshev, D., Kaibuchi, K., Alieva, I., Garcia, J. G., and Verin, A. D. (2004) Novel role of microtubules in thrombin-induced endothelial barrier dysfunction. *FASEB J.* **18,** 1879–1890
22. Tirián, L., Hlavanda, E., Oláh, J., Horváth, I., Orosz, F., Szabó, B., Kovács, J., Szabad, J., and Ovádi, J. (2003) TPPP/p25 promotes tubulin assemblies and blocks mitotic spindle formation. *Proc. Natl. Acad. Sci. U.S.A.* **100,** 13976–13981
23. Vincze, O., Tökési, N., Oláh, J., Hlavanda, E., Zotter, A., Horváth, I., Lehotzky, A., Tirián, L., Medzihradszky, K. F., Kovács, J., Orosz, F., and Ovádi, J. (2006) Tubulin polymerization promoting proteins (TPPPs). Members of a new family with distinct structures and functions. *Biochemistry* **45,** 13818–13826
24. Acevedo, K., Li, R., Soo, P., Suryadinata, R., Sarcevic, B., Valova, V. A., Graham, M. E., Robinson, P. J., and Bernard, O. (2007) The phosphorylation of p25/TPPP by LIM kinase 1 inhibits its ability to assemble microtubules. *Exp. Cell Res.* **313,** 4091–4106
25. Tokési, N., Lehotzky, A., Horváth, I., Szabó, B., Oláh, J., Lau, P., and Ovádi, J. (2010) TPPP/p25 promotes tubulin acetylation by inhibiting histone deacetylase 6. *J. Biol. Chem.* **285,** 17896–17906
26. Heng, Y. W., Lim, H. H., Mina, T., Utomo, P., Zhong, S., Lim, C. T., and Koh, C. G. (2012) TPPP acts downstream of RhoA-ROCK-LIMK2 to regulate astral microtubule organization and spindle orientation. *J. Cell Sci.* **125,** 1579–1590
27. Foletta, V. C., Lim, M. A., Soosairajah, J., Kelly, A. P., Stanley, E. G., Shannon, M., He, W., Das, S., Massague, J., and Bernard, O. (2003) Direct signaling by the BMP type II receptor via the cytoskeletal regulator LIMK1. *J. Cell Biol.* **162,** 1089–1098
28. O'Reilly, L. A., Cullen, L., Moriishi, K., O'Connor, L., Huang, D. C., and Strasser, A. (1998) Rapid hybridoma screening method for the identification of monoclonal antibodies to low-abundance cytoplasmic proteins. *BioTechniques* **25,** 824–830
29. Shevchenko, A., Tomas, H., Havlis, J., Olsen, J. V., and Mann, M. (2006) In-gel digestion for mass spectrometric characterization of proteins and proteomes. *Nat. Protoc.* **1,** 2856–2860
30. Harrison, B. A., Whitlock, N. A., Voronkov, M. V., Almstead, Z. Y., Gu, K. J., Mabon, R., Gardyan, M., Hamman, B. D., Allen, J., Gopinathan, S., McKnight, B., Crist, M., Zhang, Y., Liu, Y., Courtney, L. F., Key, B., Zhou, J., Patel, N., Yates, P. W., Liu, Q., Wilson, A. G., Kimball, S. D., Crosson, C. E., Rice, D. S., and Rawlins, D. B. (2009) Novel class of LIM-kinase 2 inhibitors for the treatment of ocular hypertension and associated glaucoma. *J. Med. Chem.* **52,** 6515–6518
31. Kang, J. H., Jiang, Y., Toita, R., Oishi, J., Kawamura, K., Han, A., Mori, T., Niidome, T., Ishida, M., Tatematsu, K., Tanizawa, K., and Katayama, Y. (2007) Phosphorylation of Rho-associated kinase (Rho-kinase/ROCK/ROK) substrates by protein kinases A and C. *Biochimie* **89,** 39–47
32. Kang, J. H., Asai, D., Tsuchiya, A., Mori, T., Niidome, T., and Katayama, Y. (2011) Peptide substrates for Rho-associated kinase 2 (Rho-kinase 2/ROCK2). *PLoS ONE* **6,** e22699
33. Hlavanda, E., Kovács, J., Oláh, J., Orosz, F., Medzihradszky, K. F., and Ovádi, J. (2002) Brain-specific p25 protein binds to tubulin and microtubules and induces aberrant microtubule assemblies at substoichiometric concentrations. *Biochemistry* **41,** 8657–8664
34. Ikegami, T., Nakamura, M., Yamane, J., Katoh, H., Okada, S., Iwanami, A., Watanabe, K., Ishii, K., Kato, F., Fujita, H., Takahashi, T., Okano, H. J., Toyama, Y., and Okano, H. (2005) Chondroitinase ABC combined with neural stem/progenitor cell transplantation enhances graft cell migration and outgrowth of growth-associated protein-43-positive fibers after rat spinal cord injury. *Eur. J. Neurosci.* **22,** 3036–3046
35. Hlavanda, E., Klement, E., Kókai, E., Kovács, J., Vincze, O., Tökési, N., Orosz, F., Medzihradszky, K. F., Dombrádi, V., and Ovádi, J. (2007) Phosphorylation blocks the activity of tubulin polymerization-promoting protein (TPPP). Identification of sites targeted by different kinases. *J. Biol. Chem.* **282,** 29531–29539
36. Wu, Y., Song, S. W., Sun, J., Bruner, J. M., Fuller, G. N., and Zhang, W. (2010) IIp45 inhibits cell migration through inhibition of HDAC6. *J. Biol. Chem.* **285,** 3554–3560
37. Lafarga, V., Aymerich, I., Tapia, O., Mayor, F., Jr., and Penela, P. (2012) A novel GRK2/HDAC6 interaction modulates cell spreading and motility. *EMBO J.* **31,** 856–869
38. Saji, S., Kawakami, M., Hayashi, S., Yoshida, N., Hirose, M., Horiguchi, S., Itoh, A., Funata, N., Schreiber, S. L., Yoshida, M., and Toi, M. (2005) Significance of HDAC6 regulation via estrogen signaling for cell motility and prognosis in estrogen receptor-positive breast cancer. *Oncogene* **24,** 4531–4539
39. Zohrabian, V. M., Forzani, B., Chau, Z., Murali, R., and Jhanwar-Uniyal, M. (2009) Rho/ROCK and MAPK signaling pathways are involved in glioblastoma cell migration and proliferation. *Anticancer Res.* **29,** 119–123
40. Kruger, J. S., and Reddy, K. B. (2003) Distinct mechanisms mediate the initial and sustained phases of cell migration in epidermal growth factor receptor-overexpressing cells. *Mol. Cancer Res.* **1,** 801–809